Population transfer between valence states via autoionizing states using two-color ultrafast π pulses in XUV and the limitations of adiabatic passage

X. Li,[1] C. W. McCurdy,[2,1] and D. J. Haxton[1]

[1]*Chemical Sciences and Ultrafast X-ray Science Laboratory, Lawrence Berkeley National Laboratory, Berkeley, California 94720, USA*
[2]*Department of Chemistry, University of California, Davis, California 95616, USA*

Population transfer between two valence states of the Li atom with a Raman process via intermediate autoionizing states well above the ionization threshold is investigated using a recently developed implementation of the muticonfiguration time-dependent Hartree Fock method. It is found that a properly chosen sequence of pump and Stokes π pulses can yield a population transfer efficiency of 53% at relatively low intensities, while the extension of the stimulated Raman adiabatic passage (STIRAP) approach to the XUV in this case is far less efficient and loses its characteristic robustness at high intensities. A rule of thumb for when STIRAP is practical is given, suggesting that at still shorter wavelengths STIRAP may be possible.

A goal for new sources of intense ultrashort pulses in the extreme ultraviolet (XUV) and x-ray regimes is to enable experiments in which a molecule is excited to an autoionizing state and then deexcited by stimulated Raman emission to construct a wave packet of valence states that is subsequently probed by other pulses [1,2]. Such experiments would address the core or inner valence levels of atoms in a chemically selective way, opening the door to new kinds of spectroscopy that create localized valence excitations in large molecules. Sufficiently intense, coherent, ultrashort x-ray pulses required by such experiments are not yet available, but the first steps towards this goal can be taken in model systems using intense ultrashort XUV pulses at the frontier of current technologies.

However, the use of ionizing radiation and Auger-decaying intermediate states opens a range of competing loss mechanisms for these sorts of nonlinear spectroscopies, and there are serious questions about their ultimate feasibility. Here we investigate a prototype of such a process in the lithium atom in *ab initio* calculations that include all the loss mechanisms that can contribute, correctly treating all the ionization continua involved as well as electron correlation during the pulses. Effecting population transfer within the lifetimes of Auger-decaying states can require pulses and delays of the order of femtoseconds, and that is the regime we explore.

Controlling the transfer of population between discrete quantum states has been the central subject of a large number of theoretical and experimental investigations in physics and chemistry [3,4], including the control of molecular dynamics and chemical reactions [5]. Stimulated Raman transitions in particular provide a powerful tool for laser manipulation of cold atoms and ions [6]. For population control, such processes have generally been implemented using nonionizing radiation, i.e., in the infrared or visible regions where intense, coherent laser pulses are available. However, the advent of coherent femtosecond and attosecond pulses [7] in the UV and XUV regimes, as well as the prospects for more intense coherent sources in both the UV and the x-ray regimes, make it interesting to extend these ideas to shorter-wavelength regimes. Although near-UV pulses have been used to drive such transitions (e.g., Ref. [8]), in general no ionization has been involved and the pulse durations were on the nanosecond scale.

In addition to searching for optimal pulses to be used in a stimulated Raman transition, it is also interesting to test the limit of an important example of such techniques, Stimulated Raman adiabatic passage (STIRAP), which was initially studied more than two decades ago [9,10]. This scheme, which makes use of two coherent laser pulses applied in a *counterintuitive* sequence, has been proven to be both effective and robust for complete population transfer between two states via an intermediate excited state. The STIRAP scheme aims at having the system adiabatically follow a specific field-dressed state, a *dark* state, achieving complete transfer of population after both pulses are terminated. These concepts have been widely used in the theory of other spectroscopic phenomena, such as Autler-Townes splitting [11], electromagnetically induced transparency [12], and coherent population trapping (CPT) [13].

In this work, we use the multiconfiguration time-dependent Hartree Fock (MCTDHF) method, previously explored and developed by several groups [14–20], to investigate the dynamics of the nonperturbative Raman process of transferring population between two valence states via a core-hole state with ultrafast coherent XUV pulses. These calculations do not depend on models of the processes in terms of a finite number of atomic states, and they include the single- and multiple-ionization continua essentially exactly. We present results for the Raman transition in atomic lithium depicted schematically in Fig. 1. Two UV pulses, centered at 58.9 and 55.5 eV, are used to transfer population from the ground $[1s^2 2s\ ^2S]$ state, via the core-hole $[1s\ (2s2p\ ^3P)\ ^2P]$ state at 58.9 eV, to the valence excited $[1s^2 3s\ ^2S]$ state. A neighboring core-hole state $[1s\ (2s2p\ ^1P)\ ^2P]$ with a different spin coupling between valence electrons, at 60.4 eV, is barely populated by the pulses we use. In this process, the desired optical excitation and deexcitation and population loss due to photoionization of all the states involved, as well as autoionization of the core-hole states, can compete to complicate this nonlinear process.

In the following we first briefly describe the MCTDHF method. Next, we describe the three-level model and the nonlinear optimization with which we found the pulses to be used in the MCTDHF calculations. We then describe the results of converged MCTDHF calculations using this pulse sequence,
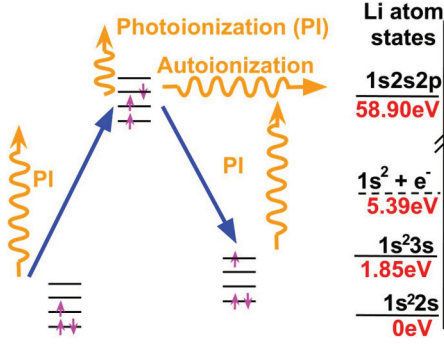
FIG. 1. (Color online) Schematic diagram of the population transfer process with the intermediate state embedded in the ionization continuum.

and of similar calculations showing the limited efficiency and robustness of the STIRAP process for this transfer of population. Finally, we propose a rule of thumb to determine whether the STIRAP method should be expected to work for effective population transfer with ultrafast XUV pulses.

MCTDHF approach. In order to properly describe stable valence states, core-hole states, and the photoionization continuua, which are all involved in this Raman process, we use a recently developed implementation of the MCTDHF method described at length previously [21,22]. The wave function is a full configuration-interaction expansion with time-dependent coefficients of Slater determinants of orbitals which are themselves time dependent. As more orbitals are included, the MCTDHF wave function converges to the exact many-electron solution. This implementation solves the time-dependent Schrödinger equation in full dimensionality, and because it is based on a combination of the discrete-variable representation (DVR) and exterior complex scaling (ECS) of the electronic coordinates, it rigorously treats the ionization continua for both single and multiple ionization.

We begin with a representation of the initial ground state and propagate the wave function while the pulses are on. We project the time-dependent total wave function onto the time-independent bound-state wave functions, computed using the multiconfiguration self-consistent field (MCSCF) method, to obtain their populations,

$$P_i(t) \equiv \left| \langle \Psi(t) | \psi_i^{(\mathrm{MCSCF})} \rangle \right|^2. \tag{1}$$

The resonance state is also represented by an MCSCF wave function, which in this approximation has a real energy.

The results presented here were calculated using ten orbitals, which can be initially labeled as $1s$, $2s$, $2p$, $3s$, $3p$, and $3d_0$. These calculations have a spin-adapted doublet configuration space of dimension 162. We use an angular DVR grid of five points in θ and a radial grid with 12 grid points per finite element. Ten finite elements were used, the first of length $2.0a_0$ providing a dense grid to represent the $1s$ orbital and orbital cusps, with five subsequent elements of length $8.0a_0$. ECS is applied to the remaining four elements extending an additional $64a_0$ with a scaling angle of 0.40 rad.

Three-level model. We first develop a simple three-level model that compares well with the accurate MCTDHF calculations and can be used to optimize pulse sequences and

interpret the mechanisms underlying the population dynamics. In this three-level system the total wave function is expanded as

$$\Phi(t) = c_{gr}(t)|\mathrm{gr}\rangle + c_{ex}(t)|\mathrm{ex}\rangle + c_{ms}(t)|\mathrm{ms}\rangle, \tag{2}$$

where $|\mathrm{gr}\rangle$, $|\mathrm{ex}\rangle$, and $|\mathrm{ms}\rangle$ are the initial ground state, the intermediate excited state, and the target metastable state, respectively, and $c_g(t)$, $c_{ex}(t)$, and $c_{ms}(t)$ are the associated time-dependent coefficients. By using the proper rotating frame, we define $b_{gr}e^{-i(E_{gr}+\Delta_p)t} \equiv c_{gr}$, $b_{ex}e^{-i(E_{ex})t} \equiv c_{ex}$, and $b_{ms}e^{-i(E_{ms}+\Delta_S)t} \equiv c_{ms}$, where E_{gr}, E_{ex}, and E_{ms} are the energies of the states of the field-free Hamiltonian. These redefined coefficients are subject to the time-dependent Schrödinger equation in the interaction picture, $i\dot{\vec{b}}(t) = \hat{H}(t)\vec{b}(t)$, where $\vec{b} = \{b_{gr}(t), b_{ex}(t), b_{ms}(t)\}$. By invoking the rotating-wave approximation, we arrive at the Hamiltonian for pump and Stokes interactions $-\mathcal{E}_p(t) \cdot \mathbf{d}_p \cos(\omega_p t)$ and $-\mathcal{E}_S(t) \cdot \mathbf{d}_S \cos(\omega_S t)$,

$$\hat{H}(t) = \begin{bmatrix} \Delta'_p - i\Gamma_1 & -\Omega_p(t) & 0 \\ -\Omega_p(t) & -i\Gamma_2 & -\Omega_S(t) \\ 0 & -\Omega_S(t) & \Delta'_S - i\Gamma_3 \end{bmatrix}, \tag{3}$$

where $\Delta'_{p,S}$ include ac Stark shifts proportional to the field intensity, and $\Omega_{p,S}(t) \equiv \mathcal{E}_{p,S}(t) \cdot \mathbf{d}_{p,S}$ denote the time-dependent Rabi frequencies for the pump (p) and Stokes (S) pulses defined by the electric-dipole-interaction approximation. Three dominant loss mechanisms due to ionization are explicitly present in this Hamiltonian, Γ_1, Γ_2, and Γ_3. Here, the decay terms Γ_1 and Γ_3, which describe the population loss process for the valence states, result from the one-photon photoionization by the intense fields; while the decaying term Γ_2 depends on both the autoionization and the two-photon ionization processes. The Auger-decay rate for the intermediate state [$1s$ $(2s2p\ ^3P)\ ^2P$] has been measured as $4 \times 10^{12}/\mathrm{s}$ [23] and our MCTDHF calculation yields $8 \times 10^{12}/\mathrm{s}$ (six orbitals), both of which are far slower than the Raman process in this study. Thus, all major population loss channels in this study are due to direct photoionization processes. By invoking the Markovian approximation, which states that the photoionization process is irreversible, one can derive that rate for each state as

$$\Gamma_{PI}(t) = \frac{3c\sigma}{4\pi^2\omega}\mathcal{E}^2(t) = \frac{3\sigma I(t)}{8\pi\omega\varepsilon_0}, \tag{4}$$

which depends on the time-dependent laser intensities [24]. Here, the integral photoionization cross section σ depends on the system and the laser wavelength. For the lithium atom, the two laser fields are in the 55 to 60 eV range of the ionization continuum, where the cross section is in the range of 0.06 to 0.07 Mb [25].

In order to enhance the population transfer efficiency, i.e., the final population remaining in the metastable state when both pulses are terminated, we vary the central frequencies, the pulse delay, and the intensities of two ultrafast XUV pulses, given a specific pulse duration. To achieve this, a nonlinear optimization of the pulse configurations with these five variables is performed using standard methods [26] to maximize the transfer efficiency. It is found that, for almost all pulse durations considered, where the temporal full width at half maximum (FWHM) of the pulse is restricted to be smaller than 10 fs, a $\pi + \pi$ pulse scheme is optimal. Here, a π pulse
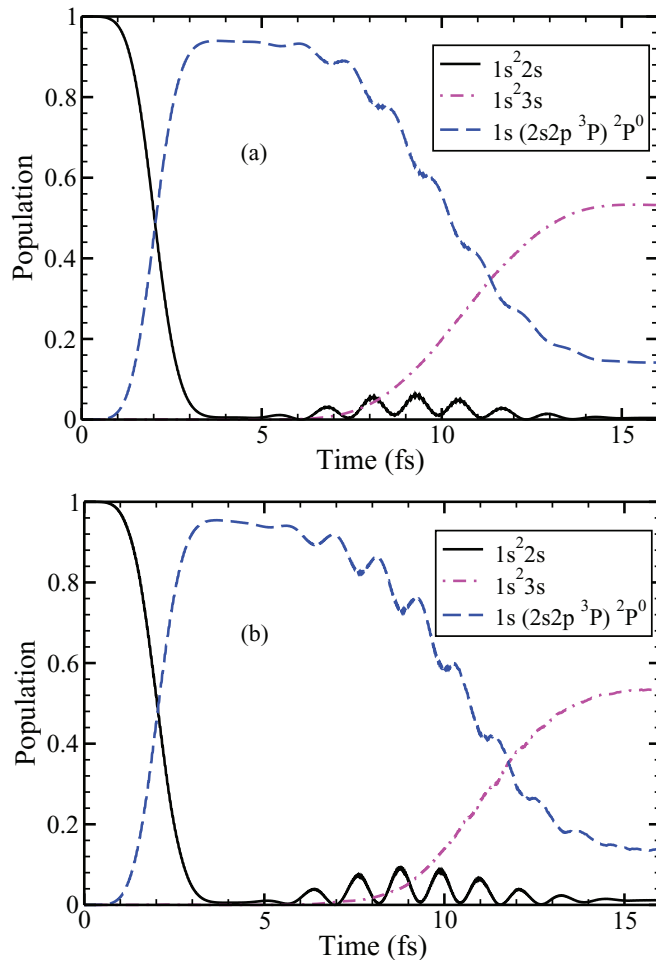
FIG. 2. (Color online) Population dynamics for (a) the three-level model simulation results and (b) MCTDHF results, with the $\pi + \pi$ pulse configuration.

FIG. 3. (Color online) MCTDHF simulation results: (a) Population transfer efficiency as a function of the Stokes pulse intensities (peak value). Filled circles: $\pi + \pi$ pulse configuration. Filled squares: STIRAP configuration. Chained vertical line denotes the adiabatic limit. (b) Population dynamics for the STIRAP configuration with time delay of $t_S - t_p = 3$ fs.

is defined such that $\int \Omega_{p,S}(t)dt = \pi$. In such a scheme, a π pump pulse is immediately followed by a π Stokes pulse, and the temporal overlap between the two pulses is zero. When no additional loss mechanisms exist in Eq. (3), i.e., $\Gamma_{1,2,3} = 0$, such a $\pi + \pi$ pulse scheme transfers 100% of the population from the initial state to the final state. As a demonstration of the $\pi + \pi$ pulse scheme when loss mechanisms are considered, i.e., $\Gamma_{1,2,3} \neq 0$, we use a set of optimized pulses with the pump having a carrier frequency of 58.9 eV, FWHM of 2 fs, and an intensity of $I_p = 9.2 \times 10^{14}$ W/cm^2, and the Stokes pulse having a carrier frequency of 55.5 eV, a FWHM of 6 fs, and an intensity of $I_S = 2.3 \times 10^{15}$ W/cm^2. The associated population dynamics of the three levels as described by Eq. (3) are shown in Fig. 2(a). The first π pulse (pump) transfers over 95% population from the ground state to the intermediate state and the subsequent π pulse (Stokes) transfers over 53% of the population to the final metastable state. The maximal decay rate in this case is approximately given as 0.1 fs^{-1} when the Stokes pulse is on, which eventually leads to a 30% loss directly to the continuum as photoelectrons.

MCTDHF results. We performed an MCTDHF calculation with the same pulse configuration used for the $\pi + \pi$ pulse scheme in Fig. 2(a). The time-dependent populations, obtained

from applying Eq. (1) to the MCTDHF wave functions, are plotted in Fig. 2(b), which confirms the results for the optimized pulses using the three-level model in Fig. 2(a). In addition, we tested the robustness of this pulse configuration by fixing the intensity ratio to be 2.3 between the Stokes and the pump pulses to optimize the transfer efficiency at $I_S = 2.3 \times 10^{15}$ W/cm^2, at which value the π pulses are defined. We then plot the transfer efficiency as a function of the Stokes pulse intensity, as shown by the filled circles in Fig. 3(a), confirming that the pulse configuration optimized by using the three-level model is indeed optimal. A second local maximum exists at a higher intensity, although the efficiency is significantly smaller than at the global maximum due to the greater photoionization loss with higher laser intensities, as described by Eq. (4).

STIRAP results. The question of population transfer via the ionization continuum using STIRAP has been investigated before [27–30], although generally in different spectral regimes and for much longer pulses than we consider here. STIRAP

via the continuum near the ionization threshold in helium has been demonstrated [31,32] with nanosecond pulses, and there have been proposals to use a third laser to suppress one of the loss channels [33]. In contrast, the present study specifically addresses the use of a core-hole autoionizing state as the intermediate state in the STIRAP process instead of population transfer via a continuum—in a spectral regime where the photoionization cross sections are about 20 times smaller than near threshold for this case. Nonetheless, as we will see, some of the loss mechanisms identified in these previous studies [28,30] operate here together with a complication specific to this case, namely, direct photoionization of the metastable state itself.

To quantitatively investigate the possible limitations for the STIRAP scheme, we also perform MCTDHF calculations of the associated dynamics. The population transfer efficiency as a function of I_S is plotted by the filled squares in Fig. 3(a), where the two XUV pulses are chosen to a fixed intensity ratio of $I_S/I_p = 20$ so that $\Omega_p \approx \Omega_S$. A temporal FWHM of 6 fs is chosen for both pulses for maximal overlap. The carrier frequencies are chosen as 58.9 and 55.2 eV to maximize the transfer efficiencies at $I_S = 0.5 \times 10^{16}$ W/cm^2 and 1×10^{16} W/cm^2. In conventional STIRAP, when loss mechanisms are negligible, the robustness of the process is reflected by a plateau of high efficiency when the pulse intensity is greater than the "adiabatic limit" [34]. The three-level model with $\Gamma_{1,2,3} = 0$ empirically gives that value here as $\int \Omega_{p,S} dt \geqslant 5\pi$. Figure 3(a) shows clearly that two notable advantages of the STIRAP scheme, the high efficiency and robustness (plateau at high intensities), vanish as compared with the ideal case.

The time-dependent population transfer dynamics from the MCTDHF calculation for the STIRAP configuration with $I_S = 5.5 \times 10^{16}$ W/cm^2 at which the conventional adiabatic limit is reached are shown in Fig. 3(b). These results demonstrate that, although intended to prepare the system in the dark state, the intense Stokes pulse leads to ionization resulting in loss of the population of ground and intermediate states into the continuum before the beginning of the pumping process.

Rule of thumb. Comparison of the MCTDHF calculation and the three-level model simulation described in Eq. (3) suggests a simple rule of thumb to predict whether STIRAP will be successful with ultrashort pulses. Ideally, with no loss mechanisms, the STIRAP scheme works best above the laser intensity of the adiabatic limit. When photoionization loss is considered, this intensity requirement introduces the photoionization decay term, Γ_{PI} in Eq. (4). If $1/\Gamma_{PI}$ is significantly longer than the pulse duration, then STIRAP can be expected to provide optimal transfer efficiency and robustness at those laser intensities. In the current study, when the FWHM of the pulse is 6 fs, STIRAP in the absence of losses would work best for $I_S \geqslant 5.5 \times 10^{16}$ W/cm^2, which leads to a decay rate of $\Gamma_{PI} \geqslant 2.8$ fs^{-1}. In that case $1/\Gamma_{PI} \leqslant 0.36$ fs, which is much smaller than the pulse duration and STIRAP is expected to fail, as was verified here. On the other hand, with pulses of the same frequencies and durations but lower intensities, a simple $\pi + \pi$ pulse scheme can succeed in transferring over half the population in this case.

Finally, we note that if they involve field-dressed states in the continuum, piecewise adiabatic passage with a pulse train [35], CPT, and adiabatic rapid passage between two levels [36] should in principle be affected by these considerations. The field-dressed-state picture can break down when photoionization processes are comparable to the desired photoexcitation process. Here, an accurate, all-electrons-active *ab initio* MCTDHF calculation established definitively that this is the case for XUV processes in lithium, but the question remains open for similar processes using x-ray pulses at energies where the photoionization cross sections are smaller.

[1] J. D. Biggs, Y. Zhang, D. Healion, and S. Mukamel, J. Chem. Phys. **136**, 174117 (2012).

[2] I. V. Schweigert and S. Mukamel, Phys. Rev. Lett. **99**, 163001 (2007).

[3] S. A. Diddams, J. C. Bergquist, S. R. Jefferts, and C. W. Oates, Science **306**, 1318 (2004).

[4] M. A. Nielsen and I. L. Chuang, *Quantum Computation and Quantum Information* (Cambridge University Press, New York, 2000).

[5] M. Shapiro and P. Brumer, *Principles of the Quantum Control of Molecular Processes* (Wiley-Interscience, Hoboken, NJ, 2003).

[6] B. Shore, *Multilevel Atoms and Incoherence: The Theory of Coherent Atomic Excitation* (John Wiley & Sons, New York, 1990), Vol. 2.

[7] F. Krausz and M. Ivanov, Rev. Mod. Phys. **81**, 163 (2009).

[8] T. Halfmann and K. Bergmann, J. Chem. Phys. **104**, 7068 (1996).

[9] J. R. Kuklinski, U. Gaubatz, F. T. Hioe, and K. Bergmann, Phys. Rev. A **40**, 6741 (1989).

[10] J. Oreg, F. T. Hioe, and J. H. Eberly, Phys. Rev. A **29**, 690 (1984).

[11] S. H. Autler and C. H. Townes, Phys. Rev. **100**, 703 (1955).

[12] S. E. Harris, Phys. Today **50**(7), 36 (1997).

[13] H. R. Gray, R. M. Whitley, and J. C. R. Stroud, Opt. Lett. **3**, 218 (1978).

[14] O. E. Alon, A. I. Streitsov, and L. S. Cederbaum, J. Chem. Phys. **127**, 154103 (2007).

[15] J. Caillat, J. Zanghellini, M. Kitzler, O. Koch, W. Kreuzer, and A. Scrinzi, Phys. Rev. A **71**, 012712 (2005).

[16] T. Kato and H. Kono, Chem. Phys. **366**, 46 (2009).

[17] I. S. Ulusoy and M. Nest, J. Chem. Phys. **136**, 054112 (2012).

[18] R. P. Miranda, A. J. Fisher, L. Stella, and A. P. Horsfield, J. Chem. Phys. **134**, 244101 (2011).

[19] H. Miyagi and L. B. Madsen, Phys. Rev. A **87**, 062511 (2013).

[20] T. Sato and K. L. Ishikawa, Phys. Rev. A **88**, 023402 (2013).

[21] D. J. Haxton, K. V. Lawler, and C. W. McCurdy, Phys. Rev. A **83**, 063416 (2011).

[22] D. J. Haxton, K. V. Lawler, and C. W. McCurdy, Phys. Rev. A **86**, 013406 (2012).

[23] H. Cederquist and S. Mannervik, J. Phys. B **15**, L807 (1982).

[24] E. Frishman and M. Shapiro, Phys. Rev. A **54**, 3310 (1996).

[25] J. J. Yeh and I. Lindau, At. Data Nucl. Data Tables **32**, 1 (1985).

[26] J. J. Mor, D. C. Sorensen, K. E. Hillstrom, and B. S. Garbow, in *Sources and Development of Mathematical Software*, edited by W. J. Cowell (Prentice-Hall, Englewood Cliffs, NJ, 1984), pp. 88–111.

[27] C. E. Carroll and F. T. Hioe, Phys. Rev. A **47**, 571 (1993).

[28] T. Nakajima, M. Elk, J. Zhang, and P. Lambropoulos, Phys. Rev. A **50**, R913 (1994).

[29] C. E. Carroll and F. T. Hioe, Phys. Lett. A **199**, 145 (1995).

[30] N. V. Vitanov and S. Stenholm, Phys. Rev. A **56**, 741 (1997).

[31] T. Peters, L. P. Yatsenko, and T. Halfmann, Phys. Rev. Lett. **95**, 103601 (2005).

[32] T. Peters and T. Halfmann, Opt. Commun. **271**, 475 (2007).

[33] R. G. Unanyan, N. V. Vitanov, and S. Stenholm, Phys. Rev. A **57**, 462 (1998).

[34] K. Bergmann, H. Theuer, and B. W. Shore, Rev. Mod. Phys. **70**, 1003 (1998).

[35] E. A. Shapiro, V. Milner, C. Menzel-Jones, and M. Shapiro, Phys. Rev. Lett. **99**, 033002 (2007).

[36] J. S. Melinger, S. R. Gandhi, A. Hariharan, J. X. Tull, and W. S. Warren, Phys. Rev. Lett. **68**, 2000 (1992).